

Point-by-point Response to Reviewer's Comments

We appreciate the three reviewers for taking time to carefully review the manuscript and give detailed and constructive comments, which has greatly helped to improve this paper. Below is our point-by-point response to each comment.

Responses to the reports of Anonymous Referees #2 and #3 begin on page 11 and page 19, respectively. Response to community comments is included on page 24.

Report #1 by Anonymous Referee #1

1.) In the manuscript, the discrepancies between measured and modeled $[XO_2]$ are noted, but not fully explained. Namely, what causes the over-estimate of XO_2 in models? Any recommendations to the chemical mechanisms? Or the difference is within the measurement uncertainty, which undermines the valuableness of the XO_2 measurement? Looking at Figure 6, model sometimes is 50-60% higher than measurement. Why? The difference shown in Figure 6 seems larger than the 31% noted in the abstract. In fact, how is the “31%” calculated?

Response: We agree that the original manuscript had insufficient discussion of the model results and we have greatly expanded this portion of the manuscript in the revision. The model overestimates of peroxy radical concentrations appear to be mainly from the build-up of unmeasured photolabile carbonyls/acids within the model. To investigate this we have conducted additional model simulations and the results are discussed within a new section “Model Sensitivity” (Sect. 3.4) with additional figures added to the SI (Figures S14 – S15). We do not recommend any additional reactions to chemical mechanisms, though we suggest the potential importance of heterogeneous chemistry for concentrated smoke plumes. We find the model predictions to be sensitive to the parameters that control the first-order dilution of unmeasured species (Fig. S14), and recommend that measurements of glyoxal, methylglyoxal, and glycolaldehyde become more commonplace.

While the difference between the model and measured values falls within the combined uncertainties as stated within the text (Lines 444-447), we respectfully disagree that this undermines the value of XO_2 measurements, which are still rare and difficult. While model predictions and estimates are quite useful, they themselves include large errors. As shown in the new *Model Sensitivity* section, adjusting key parameters within the zero-dimensional model used can lead to outputs that vary by more than 30%. Similarly, the Leighton method, which is based on the assumption of photostationary state, is extremely sensitive to the accuracy of the measurements of NO , NO_2 , O_3 , and j_{NO_2} , with uncertainties that sometimes exceed 100%. Models and estimates benefit greatly by verification by direct measurements, which we attempt in the presented research. We agree that the value of model-measurement comparisons for ROx compounds will greatly benefit from reduced uncertainties in the measurement methods, which currently are largely limited by the accuracy of calibration methods.

Finally, the last comment regarding 31% stated within the abstract was initially misstated. This percentage, which should have been listed as 34% instead, is based on the average daytime regression determined using Fig. 7 (model XO_2 vs measured XO_2). We revised the abstract text to improve clarity by stating that the model predictions were “high by an average of”. Rather than stating the highest overpredictions (models that include additional BB oxidation chemistry), we state the average over-predictions for the base mechanisms of MCM and GEOS-Chem.

Revised Text:

New section: Sect. 3.4 Model Sensitivity

The final paragraph is mostly integrated from text previously included in the model P(ROx) discussions, though some text has remained in the overall modeled P(ROx) discussion with some new text added here.

There are important fundamental limitations to how well a zero-dimensional model can describe the McCall measurements. Concentrations of several radical precursors such as nitrous acid, glycolaldehyde, methylglyoxal, and glyoxal were not constrained by measurements and were instead determined by the model. For days in which dilute biomass burning plumes arrived suddenly, it is unrealistic to expect that the model can accurately determine the concentrations of these compounds which depend on the history of the air mass. XO_2 predictions are sensitive to several model inputs. Since some secondary compounds’ concentrations build up in the model and can drive significant ROx production, we explore the sensitivity of model XO_2 predictions to the first-order dilution rate constant applied to all compounds. Shortening the dilution lifetime from 24-hr to 6-hr (the minimum value suggested by Wolfe et al. (2016) decreases model XO_2 predictions and reduces the GEOS-Chem XO_2 overprediction from 20% to 2% (Fig. S15 in SI). The most important unmeasured radical precursors that are affected by this dilution are methylglyoxal, glycolaldehyde, and 4-oxo-2-pentenal due to their collective contribution to P(ROx). We also investigate model XO_2 sensitivity to NOx. Increasing NOx inputs by 50% leads to peak daily XO_2 predictions by roughly 10%.

As the 15 pptv increase in [XO_2] observed on 17 August is not captured by model simulations, we include HONO as an additional model constraint in additional GEOS-Chem simulations (see Sect. S8 of SI). Constrained HONO concentrations were determined by the product of selected $\Delta HONO/\Delta CO$ values to the measured CO mixing ratios during BB periods. To achieve a similar ~ 15 pptv XO_2 enhancement as measured during the 17 August BB event, a HONO enhancement ratio of near 3 pptv ppbv⁻¹ is required, which provides an additional 0.15 - 0.60 ppbv HONO throughout the BB period. This $\Delta HONO/\Delta CO$ value is 30 times larger than observed by Peng et al. (2020) for similarly aged plumes. While this value is likely unrealistic, larger $\Delta HONO/\Delta CO$ have been reported by Peng et al. (2020). Other unmeasured ROx precursors were likely present and at least partially responsible for the elevated XO_2 concentrations observed.

Model sensitivity to heterogeneous HO_2 uptake was also investigated. The introduction of heterogeneous losses of HO_2 had overall minimal impacts (see Fig. 7 MCM-BBVOC-het results) even though a fairly high HO_2 uptake coefficient of 0.2 was used (Abbatt et al., 2012). Heterogeneous losses decreased modeled [OH] and [XO_2] by an average of 3.4% and 2.9%, respectively, though the impact is more evident for smoke periods with elevated PM. Our analysis of HO_2 heterogeneous uptake is limited by the uncertainty in the HO_2 uptake coefficient and the specific surface area parameter. To investigate the sensitivity of model results to these parameters, these parameters were varied for several GEOS-Chem model simulations (see Figures S9 and S10 in SI). We focus our heterogeneous chemistry sensitivity tests on a 40 min period during the 17 August BB event in which OA concentrations were 30 $\mu g m^{-3}$. Inclusion of heterogeneous chemistry with standard parameter settings ($\gamma = 0.2$) leads to a 11% decrease in [HO_2], whereas use of a much higher and likely unrealistic HO_2 uptake coefficient of 0.5 resulted in a 25% HO_2 decrease. A similar HO_2 decrease results from using a higher specific surface area of 10 $m^2 g^{-1}$. Use of a smaller HO_2 uptake coefficient of 0.02 led to a nearly negligible decrease in [HO_2]. Constraining the OA concentration at 100 $\mu g m^{-3}$ for the same period - much higher than actually observed - leads to heterogeneous [HO_2] loss of 3% for an uptake coefficient of 0.02 and 30% for an uptake coefficient of 0.2. The only conditions in which heterogeneous loss of HO_2 to BB smoke would appear to be important would be for less dilute plumes ([OA] > 100 $\mu g m^{-3}$) and a high uptake coefficient ($\gamma > 0.2$).

Revised Abstract:

Ozone (O_3), a potent greenhouse gas that is detrimental to human health, is typically found in elevated concentrations within biomass burning (BB) smoke plumes. The radical species OH, HO_2 , and RO_2 (known collectively as ROx) have central roles in the formation of secondary pollutants including O_3 but are poorly characterized for BB plumes. We present measurements of total peroxy radical concentrations ($[XO_2] \equiv [HO_2] + [RO_2]$) and additional trace-gas and particulate matter measurements from McCall, Idaho during August 2018. There were five distinct periods in which BB smoke impacted this site. During BB events, O_3 concentrations were enhanced as evidenced by ozone enhancement ratios ($\Delta O_3 / \Delta CO$) that ranged up to $0.06 \text{ ppbv ppbv}^{-1}$. $[XO_2]$ was similarly elevated during some BB events. Overall, quantified instantaneous ozone production rates ($P(O_3)$) were minimally impacted by the presence of smoke as NO_x enhancements were minimal. Measured XO_2 concentrations were compared to zero-dimensional box modeling results to evaluate the effectiveness of the Master Chemical Mechanism (MCM) and GEOS-Chem mechanisms overall and during periods of BB influence. The models consistently over-estimated XO_2 with the base MCM and GEOS-Chem XO_2 predictions high by an average of 28% and 20%, respectively. One period of BB influence had distinct measured enhancements of 15 pptv XO_2 that were not reflected in the model output, likely due to the presence of unmeasured HOx sources. To our knowledge, this is the first BB study featuring peroxy radical measurements.

Additional SI Figures: Here we include Fig. 15 along with its caption. We include Figure S14 in a subsequent comment that is more directly related to that figure (model simulations using HONO constraints from selected $\Delta HONO / \Delta CO$)

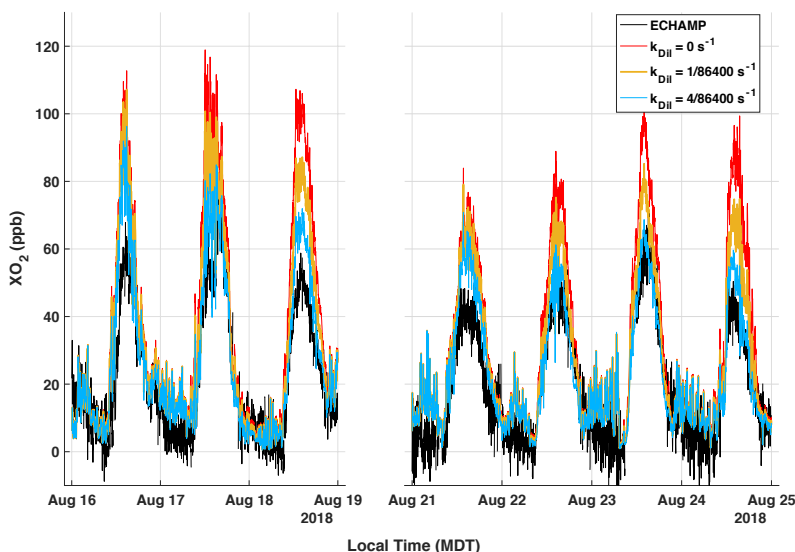


Figure S15. F0AM XO_2 predictions with varied first-order dilution rate constants (k_{Dil}) obtained using the GEOS-Chem mechanism. ECHAMP XO_2 measurements are included for comparison. Model predicted XO_2 results are shown for simulations that used the standard 24-hr dilution lifetime ($k_{Dil} = 1/86400 \text{ s}^{-1}$), a 6-hr dilution lifetime ($k_{Dil} = 4/86400 \text{ s}^{-1}$), and no dilution ($k_{Dil} = 0 \text{ s}^{-1}$).

Relevant text within SI for Fig. S15:

The sensitivity of model predicted XO_2 to the first-order dilution rate constant (k_{Dil}) was investigated using additional F0AM results acquired with the base GEOS-Chem mechanism (Fig. S15). Completely removing dilution allows for the further buildup of secondary species and higher predictions of $[XO_2]$. Increasing the rate constant from the standard 24-hr lifetime ($k_{Dil} = 1/86400 \text{ s}^{-1}$) to a 6-hr lifetime ($k_{Dil} = 4/86400 \text{ s}^{-1}$) leads to decreased XO_2 predictions that better align with the measured XO_2 values. The most important unmeasured radical precursors that are affected by this dilution setting are methyl glyoxal and glycolaldehyde. For results acquired using the MCM-BBVOC mechanism, the dilution

setting is important for additional processes including limiting the buildup of photolabile carbonyls such as 4-oxo-2-pentenal (listed as C5DICARB within MCM).

2.) The effect of HO₂ heterogeneous uptake on the radical budget is likely over-stated. As the authors noted, the HO₂ uptake coefficient is highly uncertain. A relatively large value (i.e., 0.2) is chosen. In dense BB plumes, organic aerosol is the dominant composition with mass fraction up to 80%. As discussed in Abbatt et al. 2012 and George et al., the HO₂ uptake coefficient to solid organic particles is < 0.001 and to liquid organic particles is < 0.01. If applying the small gamma values, the HO₂ heterogeneous is negligible even in dense BB plumes.

Response: We stated in our initial text that we used a fairly large uptake coefficient, so we were immediately in some agreement with this comment. Since we have already varied our uptake coefficients used for several model simulations (now shown in Fig. 9 of SI), we added additional text to clarify this issue. We now state that model results acquired using an uptake coefficient of 0.02 leads to near negligible differences when compared to models that include no heterogeneous chemistry. For our statement where we extrapolate the impact of heterogeneous chemistry to more concentrated plumes (> 100 µg m⁻³), we restate that we have used a fairly high uptake coefficient to underscore the uncertainty.

Revised Text The original paragraph focusing on heterogeneous chemistry has been mostly reworked into the new 'Model Sensitivity' Sect. 3.4 as its final paragraph (see full revised text above on page 2). This paragraph (lines 535-547) is nearly entirely revised. Included here is the most relevant text of this revised paragraph:

We focus our heterogeneous chemistry sensitivity tests on a 40 min period during the 17 August BB event in which OA concentrations were 30 µg m⁻³. Inclusion of heterogeneous chemistry with standard parameter settings ($\gamma = 0.2$) leads to a 11% decrease in [HO₂], whereas use of a much higher and likely unrealistic HO₂ uptake coefficient of 0.5 resulted in a 25% HO₂ decrease. A similar HO₂ decrease results from using a higher specific surface area of 10 m² g⁻¹. Use of a smaller HO₂ uptake coefficient of 0.02 led to a nearly negligible decrease in [HO₂]. Constraining the OA concentration at 100 µg m⁻³ for the same period - much higher than actually observed - leads to heterogeneous [HO₂] loss of 3% for an uptake coefficient of 0.02 and 30% for an uptake coefficient of 0.2. The only conditions in which heterogeneous loss of HO₂ to BB smoke would appear to be important would be for less dilute plumes ([OA] > 100 µg m⁻³) and a high uptake coefficient ($\gamma > 0.2$). Text in the conclusion has been revised (line 573). The revised portion is highlighted.

Finally, the role of heterogeneous HO₂ uptake as a ROx sink would benefit from more direct measurements of particle size distribution and knowledge of HO₂ uptake coefficients. Heterogeneous HO₂ uptake was minimal for the dilute BB plumes studied here and would appear to only be important in less dilute BB plumes if the uptake coefficient is relatively high (e.g., 0.2).

3.) Missing HONO as model input is invoked in several places as a possible reason for the model vs measurement difference, but this reasoning is questionable. First of all, the delta_HONO/delta_CO after 3hr aging of BB plume, as shown in Peng et al., is 0.1 ppt/ppb, rather than 1 ppt/ppb as quoted in the manuscript (Line 377). In addition, Peng et al. clearly stated that after 3hr the [HONO] is near or below the instrument detection limit and they refrain from interpreting what it implies in terms of potential HONO steady state in aged plumes. Lastly, HONO can be

added to the box model (using $\Delta\text{HONO}/\Delta\text{CO} = 0.1 \text{ ppt/ppb}$ and measured CO), to directly test the effect of missing HONO on the modeling results.

Response: We agree that further investigation into HONO as a potential HOx source would improve this manuscript. We have updated the typo ($1.0 \text{ pptv ppbv}^{-1}$ vs $0.1 \text{ pptv ppbv}^{-1}$) that all reviewers identified. We have included additional model simulations where we constrain HONO using CO data and selected values of $\Delta\text{HONO}/\Delta\text{CO}$, following the suggestion of Anonymous Referees #1 and #2. Due to the large discrepancy between measured and modeled XO_2 during the 17 August BB event, we specifically investigate HONO as a missing HOx precursor for this event. Simulations were run using a variety of HONO constraints (a range in $\Delta\text{HONO}/\Delta\text{CO}$ were used), and resulting XO_2 results for 17 August have been included in the SI in Fig. S14. We find a rather large $\Delta\text{HONO}/\Delta\text{CO}$ of $3.0 \text{ pptv ppbv}^{-1}$ is required for a similar XO_2 enhancement as measured. Additional text was added within our ‘Model Sensitivity’ Sect. 3.4 and is included below. We also include text added to the SI regarding the new Fig. S14. Relevant text in the SI and conclusion have also been updated accordingly.

Revised Text (Sect. 3.4, Lines 529-536):

As the 15 pptv increase in $[\text{XO}_2]$ observed on 17 August is not captured by model simulations, we include HONO as an additional model constraint in additional GEOS-Chem simulations (see Sect. S8 of SI). Constrained HONO concentrations were determined by the product of selected $\Delta\text{HONO}/\Delta\text{CO}$ values to the measured CO mixing ratios during BB periods. To achieve a similar $\sim 15 \text{ pptv}$ XO_2 enhancement as measured during the 17 August BB event, a HONO enhancement ratio of near 3 pptv ppbv^{-1} is required, which provides an additional $0.15 - 0.60 \text{ ppbv}$ HONO throughout the BB period. This $\Delta\text{HONO}/\Delta\text{CO}$ value is 30 times larger than observed by Peng et al. (2020) for similarly aged plumes. While this value is likely unrealistic, larger $\Delta\text{HONO}/\Delta\text{CO}$ have been reported by Peng et al. (2020). Other unmeasured ROx precursors were likely present and at least partially responsible for the elevated XO_2 concentrations observed.

Additional SI Figure:

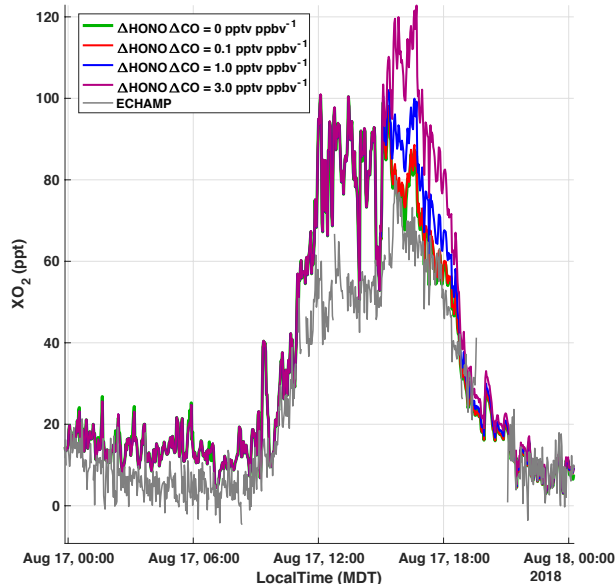


Figure S14. F0AM XO_2 predictions with constrained HONO for 17 August period. Model results were obtained using the base version of GEOS-Chem. The initial HONO data constrained is based on the model outputs of HONO acquired using GEOS-Chem. Enhancements in HONO are then added for the 17 August BB event at 15:27 MDT using HONO enhancement ratios ($\Delta\text{HONO}/\Delta\text{CO}$).

Relevant text within SI for Fig. S15:

To investigate the importance of HONO in the model results, we ran additional F0AM simulations using the GEOS-Chem mechanism with HONO concentrations constrained using a range of $\Delta\text{HONO}/\Delta\text{CO}$ values and the measured CO mixing ratios. The raw enhancements in [HONO] for this event were 0.005 – 0.020 ppbv, 0.050 – 0.200 ppbv, and 0.150 – 0.600 ppbv when the $\Delta\text{HONO}/\Delta\text{CO}$ value was set as 0.1 pptv ppbv⁻¹, 1.0 pptv ppbv⁻¹, 3.0 pptv ppbv⁻¹, respectively. XO_2 predictions for the 17 August BB event are shown in Fig. S14. In order for the model to produce the 15 pptv measured increase in [XO_2] we need to constrain HONO during BB influenced period using a rather large $\Delta\text{HONO}/\Delta\text{CO}$ of 3.0 pptv ppbv⁻¹ – much greater than the $\Delta\text{HONO}/\Delta\text{CO}$ ratios observed for similarly aged plumes by Peng et al. (2020). While this value is likely unrealistic, larger $\Delta\text{HONO}/\Delta\text{CO}$ have been reported by Peng et al. (2020) and can be implied up to 5.9 pptv ppbv⁻¹, though for considerably younger smoke plumes, using temperate forest emission factors (Akagi et al., 2011).

Additional Changes to Abstract and Conclusion: Since the HONO enhancement ratio is rather large, we remove its mention from the abstract and replace with only ‘unmeasured HOx sources’. Our statement regarding that 17 August event within the abstract has been updated:

One period of BB influence had distinct measured enhancements of 15 pptv XO_2 that were not reflected in the model output, likely due to the presence of unmeasured HOx sources.

Within the conclusion we now state the $\Delta\text{HONO}/\Delta\text{CO}$ value required for the 15 pptv rather than invoking its potential as a HOx precursor during the 17 August event (lines 565-566):

HONO photolysis likely contributed to the enhanced concentrations in [XO_2] measured during the 17 August BB period, though a rather large $\Delta\text{HONO}/\Delta\text{CO}$ value near 3.0 ppbv ppbv⁻¹ is necessary for a similar XO_2 enhancement.

4.) Figure 5 is interesting and related discussions should be expanded. For example, what does the lack of correlation between $\text{P}(\text{O}_3)$ and NO when $\text{P}(\text{ROx})$ is small suggest. Does it suggest O_3 formation is VOC-limited? More information can be distilled from the figure, or from the four variables in the figure ($\text{P}(\text{O}_3)$, $\text{P}(\text{ROx})$, NO, and HCN).

Response: We do not feel comfortable commenting on the lack of correlation in Fig. 5b ($\text{P}(\text{O}_3)$ vs NO) due to the noise associated in our $\text{P}(\text{O}_3)$ calculation. At low $\text{P}(\text{ROx})$ values, $\text{P}(\text{Ox})$ is low - typically less than 2 ppb hr⁻¹. The large variability in $\text{P}(\text{Ox})$ for this subset of data precludes making any conclusions regarding its sensitivity to [NOx].

5.) In the manuscript, some metrics are from direct measurement (e.g., [XO_2]), some metrics are calculated from measured species (e.g., $\text{P}(\text{Ox})$ from Eqn. (3)), and some metrics are purely based on box model. These need to

carefully worded in the discussion to avoid confusion. For example, Line 460 and others use the term “measured OH reactivity”, which the reader believe is the calculated OH reactivity based on measured VOCs. Then, Line 477 refers to Eqn. (3) as measured P(ROx), which makes the reader confused for a bit, as it is calculated, not measured. Such subtleties hinder the readability of the manuscript.

Response: We agree with this issue regarding the clarity of wording for metrics calculated from direct measurements. This has been addressed throughout the paper. There are two instances in which “measured OH reactivity” was mentioned (now lines 473 and 780). This wording has been changed to “OH reactivity attributed to measured compounds”. The term “measured P(ROx)” has been changed to ‘measurement-based P(ROx)’.

6.) Line 482. Are there any constraints or independent verification on the contribution of photolysis of methyl glyoxal and glycolaldehyde to the P(ROX)? Their contributions seem much larger than expected, based on measurements of these two species in previous wildfire studies.

Response: The contributions of methyl glyoxal was initially understated, and the text has been updated to state that the methyl glyoxal contributes 26% (previously listed as 19%) to the dominant ‘carbonyl + hv’ P(ROx) category. Further discussion focusing on the significant carbonyls contributing to this P(ROx) category has been added. We focus on methyl glyoxal, glycolaldehyde, and a dicarbonyl formed from BB VOC chemistry. We have included text stating that the precursors to methyl glyoxal and glycolaldehyde are from the constrained compounds of MVK/methacrolein and 2-MBO, respectively. We add context to this issue by listing concentrations of important species, and for methyl glyoxal we compare our modeled concentrations to values measured by other studies.

Revised Text:

Relevant text within our model-based P(ROx) discussion (lines 493-501) is provided with newly added lines highlighted.

Photolysis of carbonyls accounts for most of the remaining modeled daytime P(ROx), though only a fraction (less than 15%) of this category is from the measured carbonyl compounds acetaldehyde and acetone. Unmeasured carbonyls account for the rest, with methylglyoxal and glycolaldehyde accounting for 26% and 8%, respectively. Predicted methylglyoxal concentrations were typically between 0.4 and 0.6 ppbv. These concentrations are about an order of magnitude greater than those measured at mountaintop sites (Mitsuishi et al., 2018; Kawamura et al., 2013) but lower than those observed at a suburban site in China (Liu et al., 2020) and in biomass burning plumes observed in the Amazon (Kluge et al., 2020). Methylglyoxal is largely formed from the oxidation of MVK and MACR, themselves oxidation products of isoprene. A BB VOC related dicarbonyl, 4-oxo-2-pental (listed as C5DICARB within MCM), which is formed from methyl furan oxidation, accounted for 13% of P(ROx) from carbonyl photolysis.

Minor comments from Anonymous Referee #1:

Line 26-28. The reader suggests to rephrase the sentence to “the model over-estimates the XO₂ by 30%”.

Response: We have revised the abstract. The phrasing of “the model agreed within 31%” has been changed to more closely reflect this suggestion.

Revised abstract text (Lines 28-29):

The models consistently over-estimated XO_2 with the base MCM and GEOS-Chem XO_2 predictions high by an average of 28% and 20%, respectively.

Line 29-30. Suggest rephrasing to “likely due to the presence of an unmeasured HOx source that is not included in models”. The whole sentence may need to be rewritten after investigating the role of HONO as mentioned above.

Response: Since we have found that rather a large HONO enhancement ratio was required for modeling a similar XO_2 , we have updated the sentence to more closely resemble the above suggestion.

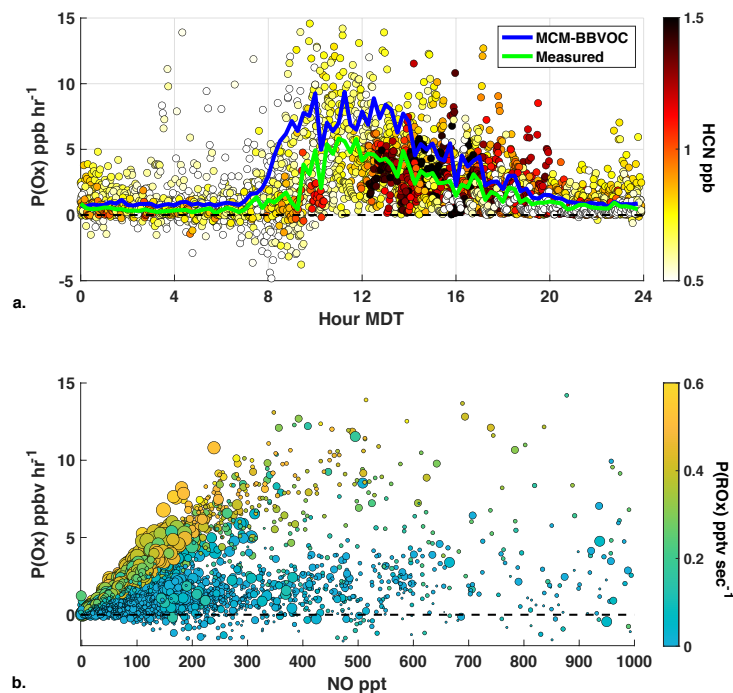
Revised Abstract Text (Lines 29-30):

One period of BB influence had distinct measured enhancements of 15 pptv XO_2 that were not reflected in the model output, likely due to the presence of unmeasured HOx sources.

Figure 5b. $\text{P}(\text{O}_3)$ is used in the y-axis, but $\text{P}(\text{Ox})$ is used in the figure caption. Be consistent.

Response: $\text{P}(\text{O}_3)$ within the figure and any mentions in the text related to Figure 5b (lines 499-502) have been updated to $\text{P}(\text{Ox})$. A similar comment from Anonymous Reviewer #2 suggested introducing a legend to figure 5a. The revised figure is presented here.

Revised Figure 5: Figure 5a with an included legend. Figure 5b with ‘ $\text{P}(\text{Ox})$ ’ replacing ‘ $\text{P}(\text{O}_3)$ ’ of y-axis title.



Line 387-397. The negative delta $\Delta O_3/\Delta CO$ on 8/16 is likely a result of inaccurate O_3 background and mixing, rather than depletion. It is because as the authors noted, the $[NO_2]$ is much smaller than $[O_3]$, suggesting that $[Ox] \approx [O_3]$, which rules out the possibility of depletion.

Response: This section (lines 399-409) has been rewritten in response to Anonymous Referee #3, but we have retained the $-0.02 \Delta O_3/\Delta CO$ value for 16 August. This $\Delta O_3/\Delta CO$ value was determined by subtracting background $[O_3]$ and $[CO]$ from plume values. Background O_3 and CO concentrations were stable. Plume concentrations (red shaded period of 16 August on period 3) also remained stable for both species for about 1 hr. Depletion of this magnitude is common for young plumes aged less than 1 day (see $\Delta O_3/\Delta CO$ table within the Jaffe and Wigder, 2012 review).

Be consistent with which model results are presented. For example, why is MCM-BBVOC-het presented in figure 8, but MCM-BBVOC in figure 6?

Response: Model results within the figures are consistently shared for MCM-BBVOC (without the additional heterogeneous chemistry) throughout the manuscript (Fig. 5 and Fig. 6). We only present MCM-BBVOC-het results in Fig. 8 to show its contribution to $L(ROx)$.

Report #2 by Anonymous Referee #2

First, the authors find that the model was not able to reproduce the XO_2 enhancement of 15 pptv during the Aug 17 smoke event, and suggested that HONO, which was not measured, may be the cause. This possibility is not really investigated in the paper. What magnitude of HONO would be needed to achieve the necessary production of XO_2 ? It would be useful for the authors to verify their assumptions by conducting sensitivity analysis of the modeled HONO (perhaps by applying a scale factor to CO or NO_2).

Response: A similar comment was made by Anonymous Reviewer #1. See the response to comment 3 on page 4 of this document. Simply put, additional model simulations were conducted using HONO concentrations that were constrained using a variety of $\Delta HONO/\Delta CO$ (ranging 0.1 up to 3.0 pptv ppbv⁻¹). We share that a $\Delta HONO/\Delta CO$ value near the 3.0 pptv ppbv⁻¹ value is required for a similar enhancement measured. As this is a rather large $\Delta HONO/\Delta CO$ value for a several hour aged plume, we suggest that the [XO_2] enhancement was likely caused by several unmeasured HOx precursors.

Second, there is an inadequate amount of discussion of how the modeled radical precursors compare to measurements. The authors showed significant model overestimates in XO_2 , P(ROx), and P(O_3) across all model mechanisms used, but did not discuss in detail the possible causes of model discrepancies. More discussion on the cause of the model overprediction and what might be pursued to reconcile the problem would be useful. Are there inaccuracies in the recycling within XO_2 species? What does the diurnal profile of model-obs discrepancy look like? What possible mechanisms could bridge the gap between measured and modelled total XO_2 ? Is the modeled NOx close to observation? How is NOx constrained in the model (e.g., kept NO/ NO_2 ratio the same as observation or not)? This kind of analysis may help better understand where the model-measurement discrepancy arises from.

Response: We agree that investigations into possible causes for the discrepancy between the measurements and models are useful. Additional model simulations have been conducted focusing on model sensitivity to a variety of parameters. We now include an additional 'Model Sensitivity' section (Sect 3.4), within the 'Results and Discussion'. The discussion of model results has been restructured to accommodate the new content and improve readability. See the page 1 response to the first Anonymous Referee #1 comment which includes the full text of Sect 3.4.

Regarding the species constrained within the model, NO and NO_2 were constrained individually – this was stated originally in the SI but additional text has been added to Sect. 2.6 'Zero-Dimensional Modeling' for clarity. Therefore, there is no model-measurement discrepancy for NOx. We have also added a list in the main text of some notable compounds constrained. Newly added Sect. 2.6 content regarding model set up is highlighted in the revised text below.

Potential causes of the model overprediction and discrepancies are introduced in Sect. 3.3 ‘Model Evaluation’ with the discussion surrounding the large contributions of unmeasured carbonyls to P(ROx) and unmeasured compounds to OH reactivity. The new ‘Model Sensitivity’ section focuses on how parameters impact as model-measurement discrepancies in XO₂. As there is a large buildup of secondary compounds, we investigate model sensitivity to the first order dilution applied to non-compounds (see time series outputs from different dilution settings in new SI Fig. S15 shown on page 3). Simulations with HONO constraints were conducted and are discussed as a potential HOx source for the 17 August event where models lacked the 15 pptv enhancement observed. We have also moved much of and expanded our heterogeneous chemistry discussion to this new ‘Model sensitivity’ section (see response to comment 2 by Referee #1 on page 4).

Revised Text:

The new Sect. 3.4 ‘Model Sensitivity’ text is included in response to Anonymous Referee #1. See page 1.

Sect. 2.6 Zero-Dimensional Modeling Revision (Lines 303-334):

We include this entire section here with newly added content highlighted.

The Framework for 0-D Atmospheric Modeling (F0AM) box model (v3.2) (Wolfe et al., 2016) was used to evaluate ECHAMP XO₂ measurements and further investigate BB impacts on instantaneous chemistry. F0AM simulations were conducted for the ECHAMP 2-minute time basis for dates in which AML concomitant measurements were present. Modeling was conducted separately for the two date ranges of interest of 16 to 18 August and 21 to 24 August then combined for analysis. We primarily focus on results acquired by employing a subset of the Master Chemical Mechanism (MCM) version 3.3.1 (Saunders et al., 2003; Jenkin et al., 2003; Jenkin et al., 2015) that included only the relevant chemical species in order to avoid unnecessary reactions and improve model time consumption. The model was constrained with all available measurements (see SI for full list), including concentrations of ozone, formaldehyde, acetaldehyde, acetone, isoprene, speciated monoterpenes, MVK, MACR, and MBO. While F0AM allows for total NO_x to be constrained, we instead constrained NO and NO₂ individually. Model results obtained using total NO_x constraints led to nearly identical daytime XO₂ predictions but with unrealistic nighttime XO₂ values. The base MCM mechanism, referred to as “MCM-base” from here on, was augmented for two additional F0AM simulations. First, the MCM-base was expanded by including additional chemistry for BB-related VOCs (referred to as “MCM-BBVOC”) of furan, methyl furan, furfural, methyl furfural, and guaiacol by manually adding the relevant chemical reactions to the MCM as detailed by Coggon et al. (2019). Second, a mechanism referred to as “MCM-BBVOC-het” included heterogeneous chemistry for HO₂ loss on organic aerosols in addition to the previously detailed BB VOC chemistry. The heterogeneous loss rates are dependent on the predicted [HO₂] values, organic aerosol surface area concentration, an uptake coefficient (γ), and mean molecular speed (Tang et al., 2014). Aerosol surface area concentrations were unmeasured and instead calculated from mass concentration measurements by applying a specific surface area. The default specific surface area was set to 4 m² g⁻¹. This setting falls slightly below the typical values measured for an urban environment of Tokyo, Japan (Hatoya et al., 2016). The default uptake coefficient was 0.20 as recommended by Jacob (2000). We explored the sensitivity of model results to both the specific surface area and uptake coefficient parameters by varying settings. We also share F0AM results acquired using the GEOS-Chem chemical mechanism. This version of the GEOS-Chem mechanism uses version 9-02 (Mao et al., 2013) with isoprene chemistry updates (Marais et al., 2016; Fisher et al., 2016; Travis et al., 2016; Kim et al., 2015). A small first-order dilution was implemented for all model experiments so that all compounds would have 24-hour lifetimes in order to prevent unreasonable accumulation of secondary species with background concentrations for all unmeasured compounds set to 0 ppbv (Wolfe et al., 2016). Concentrations of unmeasured species were also set to 0 ppbv for the model results presented in this manuscript. Minimal changes in model results were observed for additional simulations that included a “spin-up” period in order to determine initial concentrations of unmeasured compounds. As mentioned earlier, HONO is a particularly important ROx precursor in BB plumes. In addition to it not being measured during this study, the zero-dimensional models utilized cannot be expected to accurately predict HONO concentrations since

a portion of the HONO in the sampled air masses was undoubtedly emitted directly by the smoke. Furthermore, there are no HONO formation processes in the chemical mechanisms besides its homogenous formation from the reaction of OH with NO (i.e., there are no heterogeneous formation mechanisms). A complete description of our model setup, including observational constraints and uncertainties, is provided in the SI (see Sect. S7).

Last, the ozone analysis could be better utilized to reconcile the calculated rate of production with measurements. For example, the authors could show the changes in measured-to-modelled ratio of P(O₃) and XO₂ with different parameters (e.g., NO_x concentration), colored by different BB events, to find plausible explanations of the discrepancy.

Response: Our response to the previous comment discusses additional model simulations conducted to investigate overall discrepancies between the models and measured values. That response included model sensitivity to changes in parameters such as NO_x, which is suggested by this comment. Therefore, the previous response mostly covers this comment. The analysis suggested in this comment focuses on discrepancies during the BB periods. However, there were constant discrepancies during all daytime periods. The only clear additional discrepancy modeled during a BB period was the 17 August plume where the ~15 pptv XO₂ enhancement was measured only. For that discrepancy, we suggested the presence of unmeasured HO_x precursors including HONO as stated in the first response of this section.

Specific comments:

1. How does the wind speed, RH, temperature vary each day? A brief description of meteorological conditions would be helpful. Or you could add a panel for that in Fig 2.

Response: We agree that these meteorological conditions can be useful for a variety of reasons. We have included a brief mention of temperature ranges in the main text and have included a figure within the SI.

Revised Text (Lines 204-213):

Meteorological measurements were made both on the AML and permanently at the McCall site. Temperature, wind speed, and wind direction were collected by a 3-D R.M. Young (Model 81000RE) sonic anemometer stationed permanently at the McCall site at a height of 10 m. Additional wind was measured with a 2D R.M. Young (Model 81000RE) sonic anemometer mounted to the AML rooftop and corrected for speed and truck orientation with data from a Hemisphere GPS compass (model Vector V103). Temperature, RH, and wind data are shared in the supporting information (Fig. S3). Daily maximum temperatures ranged 22 °C and 28 °C while minimum temperatures ranged 4 °C to 13 °C. Solar irradiance was measured by a permanently stationed ARISense air quality sensor system (Cross et al., 2017). This was used to derive photolysis frequencies of interest, such as J_{NO_2} , by scaling measured irradiance to outputs from the National Center for Atmospheric Research (NCAR) Tropospheric Ultraviolet and Visible (TUV) radiation model. This process for deriving photolysis frequencies is described in greater detail in the supplement.

Figure S3 Added to SI

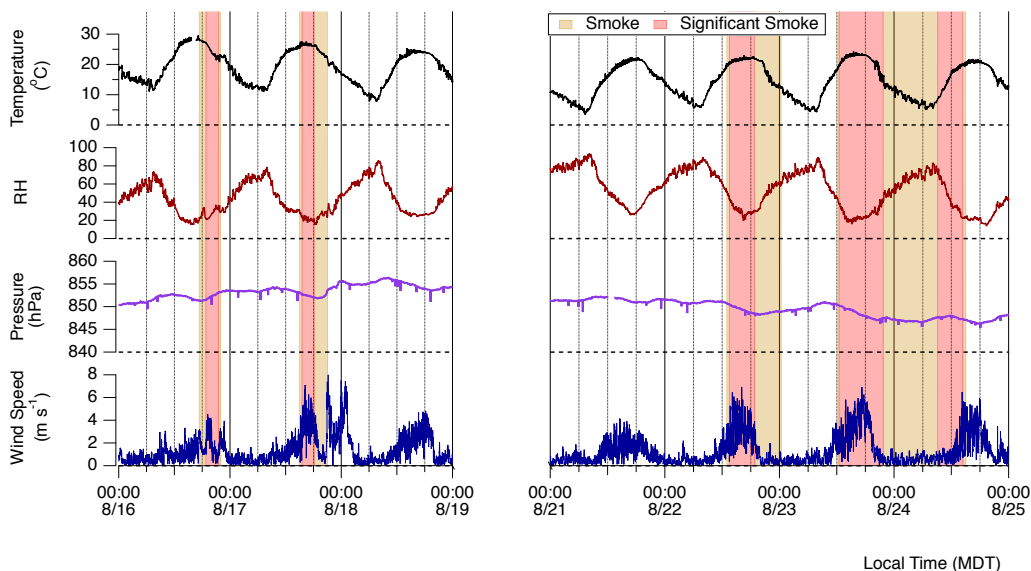


Figure S3. Meteorological data for the FIREX 2018 campaign. Periods of smoke are shaded as per Fig. 2 of the main text.

- It would be more clear if you move part of the key model description from the SI (Line S108-114) to the main text, mainly what and how the measurements were used to constrain the model and what values are used for unmeasured species.

Response: We agree that including more of the key modeling content would clear things up for the reader. We have now stated that all available measurements were used to constrain the model, and we have listed some of the more important constrained species to the main text but have kept the full list in the SI. All unmeasured species were set with initial 0 ppbv concentrations as additional simulations using a spin up period had minimal effects on our model output of interest of XO_2 . The background concentrations set for unmeasured species is now stated.

Revised Text: Revised text is listed in response to a prior comment. See the updated Sect. 2.6 ‘Zero-Dimensional Modeling’ text on page 11. New text focused on model set up is highlighted.

- Line 376-377: Peng et al. showed HONO enhancement ratios decay to ~ 0.1 ppt/ppb instead of 1 ppt/ppb for aged ($> 3\text{h}$) plumes. What enhancement ratio is needed to resolve the model disagreement if you initialize the model with HONO that scales with CO (or NO_x)?

Response: The quoted Peng et al. HONO enhancement ratio has been updated to $0.1 \text{ pptv ppbv}^{-1}$. We have included additional simulations where HONO is constrained using CO data and selected $\Delta\text{HONO}/\Delta\text{CO}$ values. $\Delta\text{HONO}/\Delta\text{CO}$ near 3 pptv ppbv^{-1} is required.

See the response to comment 3 from Anonymous Referee #1 (page 4) for greater detail and any revised text.

4. In line with the previous point, given the importance of HONO as an OH precursor, how does PO₃ change after including HONO in the model? And how does that affect NO_x? Is the estimation of the missing HONO different across different BB events?

Response: Given that we constrained NO and NO₂ individually, NO_x is not affected by any HONO constraints. Since a missing HO_x source is not as clearly evident within the other four plumes, we only focus our analysis of HONO for this one plume. P(O_x) increases by ~10% with HONO constrained using a 3.0 pptv ppbv⁻¹ enhancement ratio during that 17 August episode.

5. Figure 8: Why is the modeled P(RO_x) almost a factor of 2 larger than observed? Line 481-482 suggests that the greatest HO_x contributors in the carbonyls group are unmeasured carbonyls - how are they initialized in the model? How does each modeled radical precursor compare to the observation? Where are the sources of discrepancy in P(RO_x)? It is important to mention how the uncertainty of the carbonyls input could affect the results and conclusions.

Response: A relevant response is given to a comment focused on the verification of notable carbonyls in the model (see page 7, 'specific comment 6' of Anonymous Referee #1). There, additional text focused on P(RO_x) is included. In our initial P(RO_x) discussion, we did not mention that the overprediction of modeled P(RO_x) is for the latter half of the campaign was lower and is within ~60% of daytime measurement-based P(RO_x) (see revised text below). The unmeasured carbonyls are not initialized in the model, and we add context to their sources in our related page 7 response. Common modeled-measured radical precursors are the same due to each measured precursor being explicitly constrained, so some model overprediction in P(RO_x) is absolutely expected.

Revised Text (Line 512):

Results from the 21 August through 24 August period (see Fig. S17 in SI) are similar to the results presented above for 16 – 18 August, though the unmeasured portion of P(RO_x) is smaller for the former. This resulted from the considerably smaller concentrations of MVK, MACR, isoprene and BB VOCs measured during this period. The smaller portions for the carbonyls and 'alcohols, acids' categories led to smaller P(RO_x) totals that peaked near 0.7 pptv s⁻¹ rather than the calculated 1.2 pptv s⁻¹ for the period shown in Fig. 8.

6. Do XO₂ measurements agree with the XO₂ estimates derived from modified Leighton ratio calculated with measured ozone, NO and NO₂ concentrations from the campaign? A scatter plot of derived XO₂ versus ECHAMP observations could be made.

Response: While XO₂ estimated by the Leighton ratio (assuming photostationary state) can be useful, it is extremely sensitive to even small deviations from photostationary state (common during partially

cloudy days) and to the uncertainties in the measured values (J_{NO_2} , NO, NO_2 , and O_3) and the relevant rate constants. For typical daytime values at McCall, the combined uncertainty in XO_2 values calculated assuming photostationary state are usually greater than 100%. For this reason we have chosen not to include this line of analysis.

Minor Comments:

1. Fig 2: How is smoke presence determined? There seems to be no text descriptions.

Response: Within Fig 2., we shade red for significant smoke ($[\text{HCN}] > 1 \text{ ppbv}$) and tan for general smoke presence. There was no clear in text description for general smoke presence, so we have included an additional sentence for clarity. The general ‘smoke presence’ was identified using all Fig. 2 smoke tracers (HCN, CH_3CN , organic PM, and CO) for periods before and after the distinct BB plumes.

Revised Text (Line 227):

General smoke presence (tan shaded regions in Fig. 2) was identified before and after each significant smoke period when background smoke tracer concentrations remained elevated compared to stable background air.

2. Line 186: extra period and space

Response: This extra period and double space has been removed.

3. Line 187: missing closing parenthesis

Revised Text (Line 190):

VOC measurements were made by an ARI Vocus (proton-transfer-reaction high-resolution time-of-flight (PTR-HR-ToF) mass spectrometer) (Krechmer et al., 2018).

4. Line 302, Extra space after “MCM-base”

Response: This extra space has been fixed.

5. Line 357, sentence incomplete: “Clusters of data points at HCN concentrations ARE....”

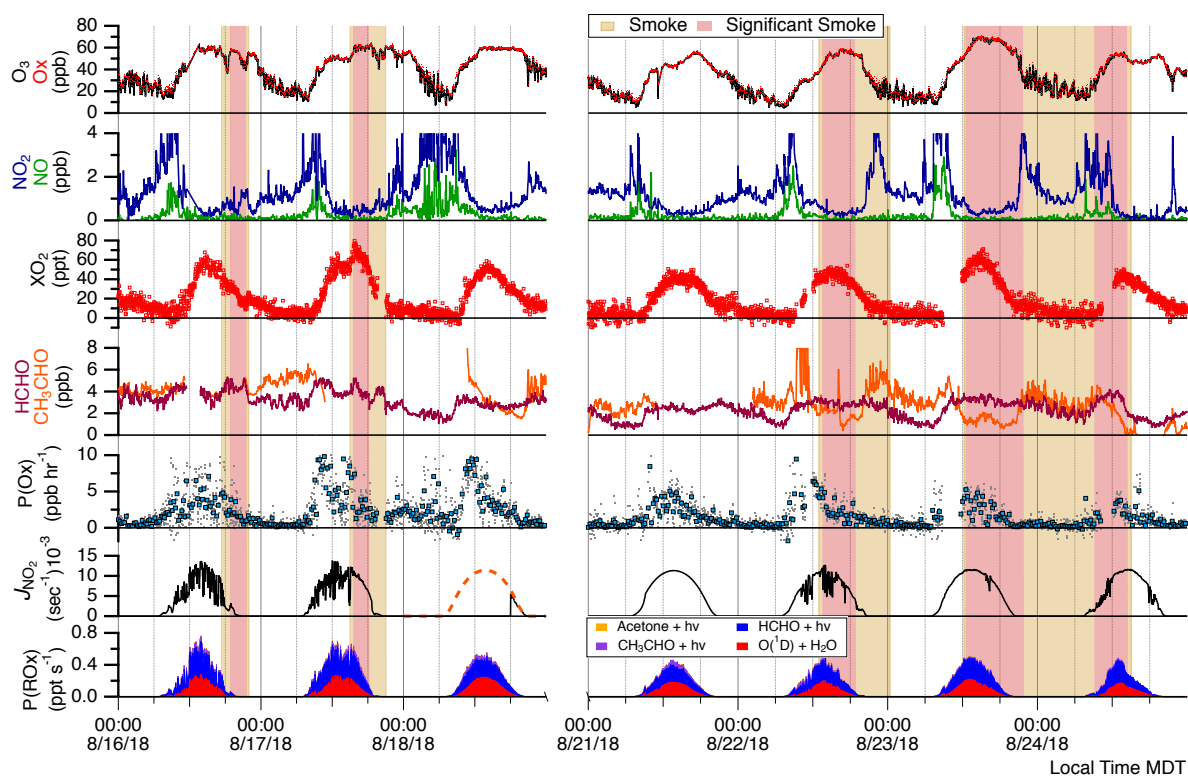
Revised text (Line 369): This has been addressed.

Clusters of data points at HCN concentrations below 0.75 ppbv are observed for the 18 August and 24 August data sets.

6. Figure 3: better have a legend for the bottom panel

Revised Figure:

Fig. 3 with the inclusion of a P(ROx) legend



7. Figure 5. Add legend for model vs obs in panel a for convenience of the readers; also specify the analysis is for Aug 17 event in the caption

Response: A legend has been added to the diurnal P(Ox) plot as requested. The caption has not been revised because this analysis includes all campaign data. As a suggestion to retitile the y-axis from Anonymous Referee #1, the revised figure that now includes a legend is shown on page.

8. Fig 6. Typo in the legend for the upper panel: ISOPO2 instead of Isoprene?

Response: The 'isoprene' XO₂ category includes ISOPO2 along with additional RO₂ species produced from isoprene oxidation. This was mentioned in the text (line 453) prior to revisions: "Modeled XO₂ comprises HO₂ (typically ~45-50%), CH₃O₂ (~20-25%), and the remaining portion a combination of CH₃CO₃, **RO₂ derived from isoprene oxidation**, and other organic peroxy radicals." We have updated the caption to Fig. 6 to avoid further confusion.

Revised Fig. 6 Caption (newly added text is highlighted):

Time series of modeled OH, HO₂, speciated RO₂, and OH reactivity (OHR). These results were acquired using the MCM-BBVOC mechanism. Periods of smoke are shaded as per Fig. 2. Measured XO₂ is included as black markers for comparison. Legend categories for XO₂ and OHR are mostly straightforward. **Note that the isoprene XO₂ category includes several RO₂ species produced from isoprene oxidation.**

9. Line 471-472: Did the decrease in OHR happen upon smoke arrival? From Fig 6 it seems to be upon smoke exit?

Response: The OHR decrease happened upon smoke departure. The text has been revised.

Revised Text (Lines 566-590):

Changes in OH reactivity were observed for some smoke periods. Subtle changes were noted during the 16 and 17 August events due to changes in the inorganic, carbonyl, biogenic, and BB VOC portions. A noticeable decrease in reactivity from 10 to $<5 \text{ s}^{-1}$ occurred on 24 August upon smoke departure. Decreases in nearly all reactivity categories contributed with notable contributions due to depletion in aldehyde concentrations and [CO]. This period sustained the lowest reactivities for the entire data set while also having the lowest concentrations of smoke tracers.

10. Line 477-478: shall be “O(1D) reaction with H₂O”

Response: This typo has been fixed. This initially read, “O(1D) reaction with O₃”.

11. SI Line 151: fix typo “GOES-Chem”

Response: This typo has been fixed to “GEOS-Chem”.

12. Fig S10 and 11: fix caption placeholder (Fig X)

Response: These placeholders have been updated to correctly reference the previous SI figure.

Point-by-point Response to Reviewer's Comments

Report #3 by Anonymous Referee #3

Major Comments:

Line 387 etc: I understand that the dO_3/dCO metric has been used before, but it seems to me that it is underconstrained here. Wouldn't the derived slope be strongly dependent on the time of day when the measurements were taken? O_3 has a strong diurnal cycle due to photochemistry, while CO does not. So across the several hours of measurements encompassing in-plume as well as pre/post plume background, the dCO term will likely be dominated by the addition of CO in vs out of the plume. However, the dO_3 term will be a sum of the O_3 added (or lost) from plume-specific chemistry plus any O_3 that would have been added (or lost) during the several hour measurement period due to regular photochemistry. With this in consideration, it appears that the slopes in Fig. S6 are most positive for the 22nd and 23rd because those data were taken during the early part of the day when ambient O_3 concentrations were increasing most rapidly, while the slope for the 17th was smaller because the data came just shortly before peak daily O_3 , and the slopes for the 24th and 16th (not shown) were smallest because the data came from after the daily peak of O_3 when mixing ratios were declining slowly. This might correlate with your calculated $P(Ox)$, though it would depend on $L(Ox)$ too I think. In other words, this method could work if it was using dO_3/dCO data that came from a short enough time span that the daily O_3 cycle was not a factor, for instance aircraft measurements spanning just a few minutes. But here, you're deriving a slope between in-plume data and out-of-plume data that are separated in time by several hours, during which time the actual O_3 in each air mass is changing (and changing in different ways depending on time of day of sampling). Therefore I do not think you can use this analysis to support your abstract-level conclusion that "During BB events, O_3 concentrations were enhanced..." at line 23. That conclusion may still be accurate, but you will need to provide better evidence.

Response: We agree that the $\Delta O_3/\Delta CO$ values we initially presented are indeed impacted by the time of day and not solely due to the impact of smoke photochemistry. The 22 August and 23 August $\Delta O_3/\Delta CO$ values are significantly affected by the increase in O_3 observed during that time of day regardless of the presence of smoke. This led to the high $\Delta O_3/\Delta CO$ values. However, we feel confident that the values we present for the smoke events of 16, 17, and 24 August can be attributed to smoke photochemistry. While the 22 August and 23 August smoke events occurred in the early afternoon with subtle changes in O_3 , the other 3 events all occurred after 15:00 MDT and had distinct and more immediate changes in O_3 . Furthermore, these events had stable levels of $[O_3]$ and $[CO]$ during both smoke and background periods. In response to this comment, we omit the $\Delta O_3/\Delta CO$ analysis for the 22 August and 23 August events, and we continue to present $\Delta O_3/\Delta CO$ for the other BB events of 16, 17, and 24 August. The text within both 'Calculations' section (Sect. 2.5) and 'Ozone Production' section (Sect. 3.2) have been updated to address these changes. Data for 22 and 23 August has been omitted from Fig. S8 (previously Fig.

S6) to reflect these changes. Within the abstract, the range in $\Delta O_3/\Delta CO$ is reported. The range in the abstract has been updated accordingly.

Revised Text (revised portions related to this comment have been revised):

Lines 271-281 (Sect. 2.5 ‘Calculations’ within Sect. 2 ‘Methods’)

Ozone enhancement ratios $\Delta O_3/\Delta CO$ from smoke influence were determined for the most distinct BB events of 16, 17, and 24 August. For the 17 and 24 August events, the ozone enhancement ratio was determined using the York bi-variate linear regression method (York et al., 2004) using a continuous section of O_3 and CO data that includes 60 minutes of background air, a transitional smoke period (tan shaded regions in Fig. 2), and 60 minutes of significant smoke period data (red shaded regions in Fig. 2). Enhancements in NO_2 were typically under 0.2 ppbv and so the difference between considering ΔO_x ($O_x = O_3 + NO_2$) and ΔO_3 was negligible. The linear regressions are included in the supplement (Fig. S8). $\Delta O_3/\Delta CO$ for the 16 August event was determined using Eq (1) with O_3 and CO data collected during a stable period at the start of the significant smoke period and a stable background prior to smoke presence.

$$\Delta O_3/\Delta CO = ([O_3]_{Smoke} - [O_3]_{Background}) / ([CO]_{Smoke} - [CO]_{Background}) \quad (1)$$

This event had a temporary depletion in O_3 by ~ 20 ppbv for the start of smoke significance, then returned to near background levels of O_3 . $\Delta O_3/\Delta CO$ values were not calculated for the remaining 22 August and 23 August smoke events. These events had less distinct O_3 enhancements and occurred at times that O_3 increased during non-smoky time periods.

Lines 399-409 (Sect. 2.5 ‘Calculations’ within Sect. 3 ‘Results and Discussion’)

We describe the extent of ozone formation for the 16 August, 17 August and 24 August BB influenced periods using the commonly used $\Delta O_3/\Delta CO$ metric. These values depict the O_3 produced in transit to the McCall site while accounting for plume dilution or overall smoke influence of the site air sampled. $\Delta O_3/\Delta CO$ values were -0.02 , 0.06 and 0.03 ppb ppbv⁻¹ for the 16, 17 and 24 August smoke events, respectively. These calculated values fall within the wide variability and range of literature $\Delta O_3/\Delta CO$ values for boreal and temperate forest fire smoke plumes aged less than two days, including numerous examples of ozone depletion for aged plumes (Jaffe and Wigder, 2012). Though the smoke was likely sourced from the same wildfire for the 16 August and 17 August events (section 2.4), we observe O_3 depletion on 16 August and O_3 enhancement on 17 August. $\Delta O_3/\Delta CO$ values were not calculated for the 22 August and 23 August smoke events as we were unable to attribute the observed increases of O_3 to smoke influence as they occurred at the same time that O_3 usually increased during non-smoky time periods as mentioned in the section 2.5. Ox enhancement ratios are not presented but differed insignificantly from O_3 enhancement ratios as NO_2 concentrations were much lower than O_3 concentrations (see Fig. 3).

Revised Figure (Fig. S8 in supplement):

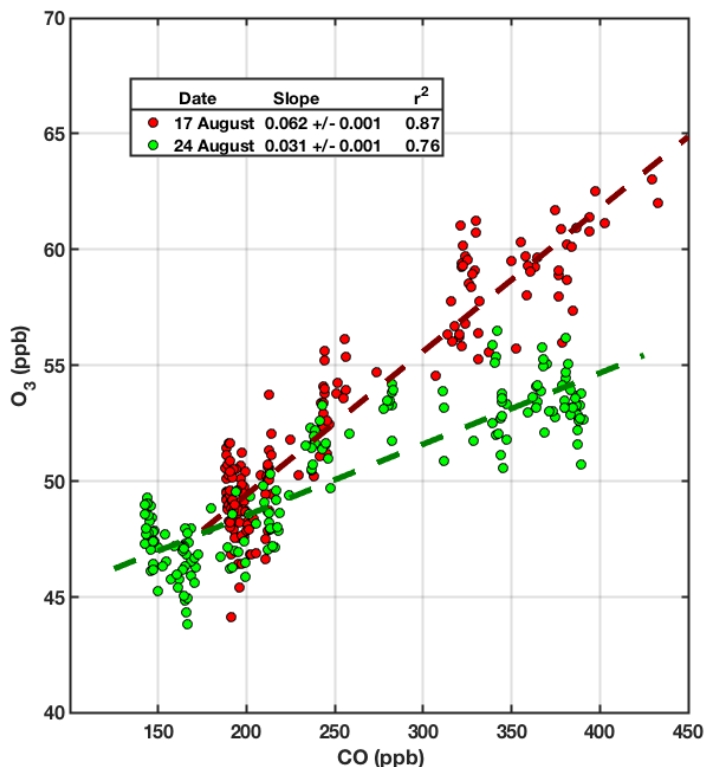


Figure S8. Comparisons of 2-minute O₃ and CO data that were used to derive biomass burning ozone enhancement ratios ($\Delta O_3/\Delta CO$) for the 17 and 24 August BB smoke events. Each set of data plotted was collected continuously and with the selected periods including 60 minutes of background air, a transition to or from BB smoke influence, and 60 minutes of significant BB smoke influence ($[HCN]>1.0$ ppb).

Fig. 4: The same analysis as my previous comment applies here; O₃ has a prominent diurnal cycle that would exist with or without a wildfire plume, while HCN would not. Plume chemistry may enhance the O₃ cycle, but it apparently doesn't dominate it. Thus, the trends shown in this plot are driven by that underlying O₃ diurnal cycle. The slopes are steep and positive for data taken when a plume arrived during midmorning when O₃ is increasing due to ambient photochemistry, and shallow for data taken when a plume arrived after peak daily O₃. If you had a plume arrive at ~midnight, O₃ would be decreasing while HCN increased, giving a negative slope in Fig. 4. Therefore I do not think you are correctly interpreting the apparent positive correlation between O₃ and HCN here. The proper correlation would be between only the O₃ derived from smoke plume chemistry (i.e. subtracting the normal background photochemical diurnal cycle) vs. HCN. Obviously that's really difficult to parse and would likely require a model, so I'm not sure what to suggest other than removing this part of the analysis.

Response: We simply use Fig. 4 (O₃ vs HCN) to show that the greatest [O₃] occurred during the smokiest periods (highest HCN values) and do not ascribe any particular meaning to the O₃/HCN ratio. The negative slope comment for regarding any possible nighttime HCN enhancements is irrelevant because Fig. 4 only includes daytime data

(9:00 to 22:00 MDT) as stated in both the text and figure caption. Therefore, we have chosen to keep this figure and respectfully disagree that it should be removed.

Line 354: Also, can you state here what is the R^2 value for the correlation in Fig. 4?

Response: As per the response to the previous comment, we are not presenting an O_3/HCN slope and merely include this plot to point out that the highest $[O_3]$ values occurred during the smokiest periods. Since we are not presenting any slopes, we think that it would be misleading to include an R^2 value as it would suggest that the correlation between O_3 and HCN should be considered overly quantitatively.

Line 376: I believe $j(HONO)$ was measured, or could be estimated. Can you do a rough calculation of how much $[HONO]$ would be needed to account for the added XO_2 ? That would be helpful for convincing the reader that it is reasonable to assume HONO is the missing factor.

Response: Similar comments have been made by Anonymous Referees #1 and #2. See our response to Anonymous Referee #1 at the end of page 4. Rather than doing a rough calculation to suggest the HONO enhancement required to achieve a 15 pptv enhancement in XO_2 , we conducted additional model simulations where a range in HONO concentrations were constrained by applying different $\Delta HONO/\Delta CO$ values. An enhancement of up to 0.6 ppbv HONO is required suggesting a $\Delta HONO/\Delta CO$ value of near 3.0 pptv ppbv⁻¹.

Line 377: The fit line from Peng et al. 2020 (Fig. 3) suggests a value of more like 0.1 pptv/ppbv⁻¹ for average $dHONO/dCO$ at 3 hours age, not 1 pptv/ppbv⁻¹ as stated here. However, the line is fit to all data regardless of in situ j_{HONO} , and some plumes did have elevated $[HONO]$ at those ages, so it's possible this plume also did.

Response: The incorrect $\Delta HONO/\Delta CO$ value of 1.0 pptv ppbv⁻¹ has been corrected to the correct value of 0.1 pptv ppbv⁻¹. We also state that Peng et al. (2020) observed a range of values (line 531): “This $\Delta HONO/\Delta CO$ value is 30 times larger than observed by Peng et al. (2020) for similarly aged plumes. While this value is likely unrealistic, larger $\Delta HONO/\Delta CO$ have been reported by Peng et al. (2020).”

Line 404: Here you say “...there is little correlation between $P(Ox)$ and smoke tracers.” Then in the next sentences you discuss examples of how BB influences $P(Ox)$. I would agree with the sentence at line 404. Also, Fig. 5a is not the correct plot to show to conclude that “ $P(Ox)$ is slightly higher during the afternoon and evening smoke influenced periods compared to non-smoke periods” as you say at line 408. I see the high $[HCN]$ data covering a similar span of $P(Ox)$ as low $[HCN]$ data. Really to draw this conclusion you would need to split the green trace

(diurnal cycle of measured P(Ox)) into two, one with high HCN and one with low HCN to show the difference between them. Please do that, and then alter the text to tell a consistent story that there either is or is not a strong effect of smoke on P(Ox) in your measurements.

Response: We agree that the original text was not written clearly. As requested, we have created a smoke P(Ox) median line ([HCN] \geq 1ppbv) and compared to a non-smoke median line ([HCN] $<$ 1ppbv). We do not include these results in the manuscript, but overall we have found negligible difference between P(Ox) for smoke and non-smoke data. The median diurnal cycles for smoke and non-smoke data are about the same at all times with the difference between smoke and non-smoke exchanging P(Ox) values alternating between negative and positive values. In response to these findings, we have slightly altered the text and have removed the previous statement that P(Ox) was greater in the afternoon and evening.

Revised Text:

Instantaneous O₃ production rates are calculated using NO and XO₂ concentrations (Fig. 3). Gaps in P(Ox) are due to measurement gaps in XO₂ when ECHAMP was offline for calibrations and diagnostic tests. The highest P(Ox) values occurred on 17 and 18 August during non-smoky periods between 10:00 MDT and 12:00 MDT, reaching formation rates slightly greater than 8 ppbv hr⁻¹. For the entire campaign, median P(Ox) peaked at 11:00 MDT at 5.8 ppbv hr⁻¹. As NO concentrations were low and rarely exceeded 1 ppbv, changes in [NO] had a near-linear impact on P(Ox). Noisy P(Ox) periods, such as the entire afternoon of 16 August, are mainly attributed to the atmospheric variability of and measurement precision for NO. Overall, there is little correlation between P(Ox) and smoke tracers. However, elevated P(Ox) during the 17 August event is somewhat evident. The ~27% increase in XO₂ and near constant value for NO led to this temporary increase in P(Ox). P(Ox) increased from ~2.5 to 8.9 ppbv hr⁻¹ during the transition from background air to significant smoke, remained elevated for 34 minutes, and then returned to near background P(Ox) rates. The overall lack of impact of BB influence on P(Ox) is further depicted in the P(Ox) diurnal cycle of Fig. 5. ~~P(Ox) is slightly higher during the afternoon and evening smoke influenced periods compared to non-smoke periods.~~ Modeled P(Ox) results for the same time period are also presented in Fig. 5a with the green median trend. These model results were acquired using F0AM with the MCM-BBVOC mechanism. Modeled P(Ox) is consistently greater than measured values with the greatest discrepancy occurring in the 7:45 to 8:15 MDT period. This difference is due to modeled [XO₂] being greater than measured [XO₂]. While we present results acquired using four unique chemical mechanisms, model predicted P(Ox) was always greater than measurements, though within the combined uncertainties.

Line 477: By plotting them together in Fig. 8, you're directly comparing measured P(ROx) from a subset of sources with modeled P(ROx) from all sources. They don't agree very well, nor should they agree, especially at night when alkenes+O₃ dominates. But this just adds confusion, and it doesn't help answer the real question of how well does the P(ROx) from measured sources compare with the P(ROx) modeled from the same subset of sources? I'd suggest maybe adding a dashed line for the P(ROx) modeled from that same subset for comparison, or altering the figure in some other way to help clarify so you're not comparing apples and oranges.

Response: The model was constrained using all available measurements. Therefore, the modeled P(ROx) is based on our measurements but also includes additional ROx precursors that the model predicts (i.e., P(ROx) from measured sources and P(ROx) modeled from the same subset of sources are exactly the same, because it is constrained that way). The model categories of ‘O(¹D) + H₂O’ and ‘HCHO + hv’ are strictly based on measurements and the carbonyl photolysis section includes photolysis of our constrained acetaldehyde and acetone measurements. The inclusion of measurement-based P(ROx) is there only to show the additional P(ROx) that is found by the model, largely due to the photolysis of unmeasured carbonyl compounds.

Minor Comments:

Line 33: add a citation here for Brazil and Australia fires

Revised text (Line 33): A citation was added for each fire.

For example, Brazil’s Amazon rainforest wildfires in 2019 (Cardil et al., 2020) and Australia’s bush fires in 2019-2020 (Yu et al., 2020) were both marked by historically high amounts of land burned.

Line 272: It would be helpful if you refer to a specific location in the SI, e.g. Sect. S4 here. Please check other references to the SI as well.

Response: This is a good suggestion. We have updated each mention of the SI so that we refer to a specific section or figure.

Fig. 5: The figure panels are labeled P(O₃), but should probably be P(O_x) to be consistent with the caption and rest of text (and be consistent throughout).

Response: The P(O₃) appearances in the text and Fig. 5 have been updated accordingly. See our page 8 response to Anonymous Referee #1 that includes the revised figure.

Line 384: I’d prefer if you labeled the green and blue traces using a legend in the figure, rather than having to dig through the caption to find that information. Same goes for the P(ROx) speciation in the bottom panel of Fig. 3.

Response: Anonymous Referee #2 has also requested figure legends. We present revised Fig. 3 and Fig. 5 on page 16 and 8, respectively.

Line 418: Model Evaluation should be Sect. 3.3, not 3.2.

Response: The ‘Model Evaluation’ section number has been updated accordingly. The numbers of sections and figures have been double checked to avoid any repeats or skips.

Community comments

'Interpretation of 2B UV absorption O₃ measurement in wildland fire plumes' by Andrew Whitehill

The manuscript claims that "O₃ was measured by a 2B-Tech UV absorption instrument." This instrument (along with most UV absorption instruments) measure ozone at 253 nm. UV photometric ozone monitors, including the 2B instruments, are known to produce significant positive interferences due to VOC's and particulate matter in wildland fire plumes. These interferences tend to be correlated with CO concentrations. The Authors do not sufficiently address this analytical artifact in the manuscript and how they corrected for or addressed it. Given that the delta O₃ vs delta CO ratio was a critical aspect of this paper, authors should provide additional description of how they corrected their O₃ measurements for fire related smoke artifacts or provide a justification for why such an artifact is not present in their data.

References to VOC and particulate artifacts in UV-photometric ozone measurements:

- Huntzicker, J. J. and Johnson, R. L., Investigation of an ambient interference in the measurement of ozone by ultraviolet absorption photometry, *Environ. Sci. Tech.*, 13, 1414–1416, 1979.
- Grosjean, D. and Harrison, J.: Response of chemiluminescence NO_x analyzers and ultraviolet ozone analyzers to organic air pollutants, *Environ. Sci. Tech.*, 19, 862–865, 1985.
- Dunlea, E. J., Herndon, S. C., Nelson, D. D., Volkamer, R. M., Lamb, B. K., Allwine, E. J., Grutter, M., Ramos Villegas, C. R., Marquez, C., Blanco, S., Cardenas, B., Kolb, C. E., Molina, L. T., and Molina, M. J.: Technical note: Evaluation of standard ultraviolet absorption ozone monitors in a polluted urban environment, *Atmos. Chem. Phys.*, 6, 3163–3180, <https://doi.org/10.5194/acp-6-3163-2006>, 2006.
- Spicer, C. W., Joseph, D. W., and Ollison, W. M.: A re-examination of ambient air ozone monitor interferences, *J. Air Waste Manage.*, 60, 1353–1364, 2010.
- Long, R. W., Whitehill, A., Habel, A., Urbanski, S., Halliday, H., Colón, M., Kaushik, S., and Landis, M. S.: Comparison of ozone measurement methods in biomass burning smoke: an evaluation under field and laboratory conditions, *Atmos. Meas. Tech.*, 14, 1783–1800, <https://doi.org/10.5194/amt-14-1783-2021>, 2021.

Response: Thank you for your comment. This is a valid point. In response, we have added content to both the main text and supplement and include a relevant figure (Figure S2 within the Supplement).

Fortunately, our ECHAMP peroxy radical sensor provides a separate measurement of Ox (Ox = O₃ + NO₂) which we can compare to the 2B O₃ measurements. In the ECHAMP inlet, ambient air is mixed with excess NO which reacts with O₃ to form NO₂ which is later quantified by an Aerodyne CAPS sensor based on absorption of light at 450 nm. Unlike the 254 nm absorption bandpass used by the UV absorption method, few compounds absorb in this blue region of the spectrum and so these positive interferences are expected to be minimal (Kebabian et al., 2008). In new SI Figure S2, we share a time series of both the 2B O₃ and one of the CAPS Ox results. For a more direct comparison, we added NO₂ (measured separately by TILDAS) to our 2B O₃ measurement to generate concentrations of Ox. The 17 August period shown includes a non-smoke period followed by a smoke period that starts at about 15:30 local time. The CAPS instrument went offline for diagnostic purposes at 19:30. Organic PM mass concentrations increased from ~10 ug m⁻³ to 30 ug m⁻³ upon smoke influence. There is good agreement between the 2B derived Ox and CAPS Ox during both the smoke and non-smoke periods for both this period shown and for the entire campaign, indicating that interferences in the 2B Tech O₃ instrument were minimal. This is not surprising as the smoke plumes we sampled were more dilute than those considered by Long et al. (2021). Here, the smoke plumes led to CO enhancements of near 100 ppb, whereas the smoke plumes studied by Long et al. (2021) had CO concentrations of several parts per million.

References:

- Kebabian, P. L., Wood, E. C., Herndon, S. C., and Freedman, A.: A practical alternative to chemiluminescence-based detection of nitrogen dioxide: Cavity attenuated phase shift spectroscopy, *Environmental science & technology*, 42, 6040-6045, 2008.

Revised text

Main text (line 188)

While particulate matter and VOCs can positively interfere with photometric O₃ measurements (Huntzicker and Johnson, 1979; Long et al., 2021), comparison to a separate Ox measurement revealed minimal interferences in the 2B-Tech O₃ observations (see Sect. S2 of SI).

Supplement (new section has been added: S2 Supplementary Measurements)

S2 Supplementary Measurements

Photometric O₃ monitors can suffer from interferences from VOCs and PM that absorb or scatter 254 nm UV radiation (Huntzicker and Johnson, 1979). Recent measurements in concentrated BB plumes ([CO] > 1 ppmv) have shown that this interference can be large for certain types of photometric O₃ measurements (Long et al., 2021). The potential for our O₃ measurements, collected using a 2B-Tech Model 205 UV absorption monitor, to be impacted is low given that we sampled dilute BB plumes in this study (enhancements of PM < 30 μg m⁻³ and [CO] < 0.1 ppmv). Furthermore, a comparison of the 2B O₃ measurements to separate Ox measurements made by our novel ECHAMP XO₂ sensor demonstrate that interferences are negligible. ECHAMP measures Ox by mixing ambient O₃ with excess NO to form NO₂ which is later quantified by CAPS NO₂ instruments. The CAPS Ox results are based on the absorption of light at 450 nm and are expected to have minimal interferences as few compounds absorb in this region (Kebabian et al., 2008). We show a time series of 2B-Tech O₃ and ECHAMP Ox measurements in Fig. S2. The Ox measurements only include up to 2 ppbv NO₂, and a separate Ox time series derived from adding the 2B-Tech O₃ with TILDAS NO₂ data is shown for a more direct comparison to the ECHAMP CAPS Ox data. The 17 August period includes nearly 15 hours of background air and a nearly 3-hour smoke influenced period that started at 15:27 MDT and included enhancements of ~100 ppbv CO and ~20 μg m⁻³ organic PM. The 2B O₃ data during both the background and smoke periods, as well as for the entire campaign, agree with the CAPS Ox acquired from ECHAMP.

New Figure included in Supplement:

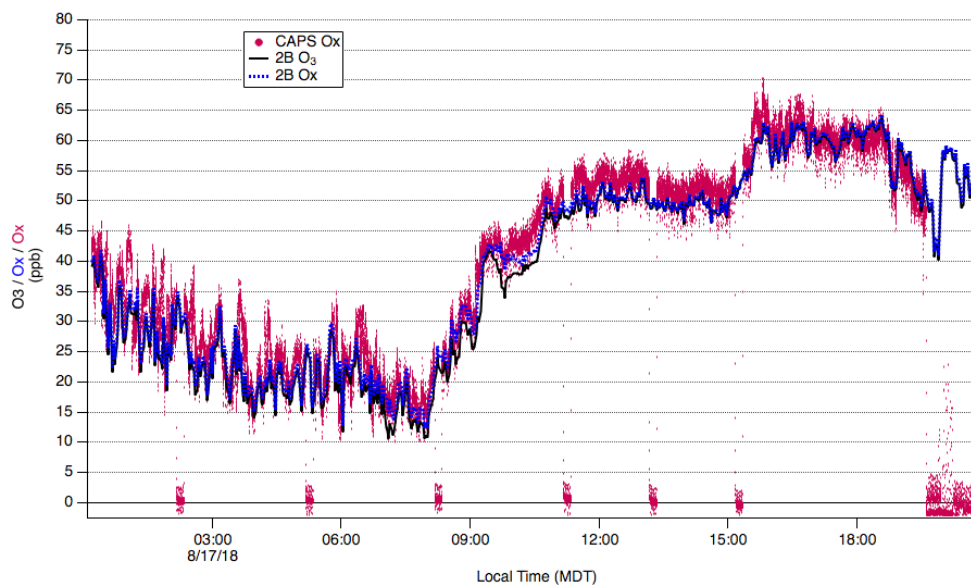


Figure S2. Time Series of 2B-Tech O₃, 2B-Tech derived Ox, and CAPS Ox data acquired from ECHAMP XO₂ sensor.